Lubrication by charged polymers

Uri Raviv[1], Suzanne Giasson[2], Nir Kampf[1], Jean-François Gohy[3], Robert Jérôme[3] & Jacob Klein[1,4]

[1]*Weizmann Institute of Science, Rehovot 76100, Israel*
[2]*Department of Chemistry and School of Pharmacy, University of Montreal, Québec, Canada H3C 3J7, and CERSIM, Laval University, Québec, Canada G1K 7P4*
[3]*Center for Education and Research on Macromolecules, University of Liège, Sart-Tilman B6, 4000 Liège, Belgium*
[4]*Physical and Theoretical Chemistry Laboratory, Oxford University, South Parks Road, Oxford OX1 3QZ, UK*

Long-ranged forces between surfaces in a liquid control effects from colloid stability[1] to biolubrication[2], and can be modified either by steric factors due to flexible polymers[3], or by surface charge effects[4]. In particular, neutral polymer 'brushes' may lead to a massive reduction in sliding friction between the surfaces to which they are attached[5–7], whereas hydrated ions can act as extremely efficient lubricants between sliding charged surfaces[8]. Here we show that brushes of charged polymers (polyelectrolytes) attached to surfaces rubbing across an aqueous medium result in superior lubrication compared to other polymeric surfactants. Effective friction coefficients with polyelectrolyte brushes in water are lower than about 0.0006–0.001 even at low sliding velocities and at pressures of up to several atmospheres (typical of those in living systems). We attribute this to the exceptional resistance to mutual interpenetration displayed by the compressed, counterion-swollen brushes, together with the fluidity of the hydration layers surrounding the charged, rubbing polymer segments. Our findings may have implications for biolubrication effects, which are important in the design of lubricated surfaces in artificial implants, and in understanding frictional processes in biological systems.

Normal and shear forces between mica surfaces immersed in water were measured using a surface force balance (SFB) described earlier[9] (Fig. 1 bottom inset). Control measurements were carried out in salt-free water, revealing the long-ranged repulsion due to counterion osmotic pressure followed by a jump, on approach, into adhesive contact, in agreement with earlier observations[10,11]. The mica surfaces were then made hydrophobic ('hydrophobized'), as described elsewhere[12], by coating with a layer of stearic trimethylammonium iodide (STAI: $CH_3(CH_2)_{17}N^+(CH_3)_3I^-$), and on approach across water jumped into a strongly adhesive contact due to the hydrophobic attraction between the STAI layers[13] (Fig. 1 top inset). Finally, polyelectrolyte (PE) brushes were created on the hydrophobized mica using the diblock copolymer poly(methyl methacrylate)-*block*-poly(sodium sulphonated glycidyl methacrylate) copolymer (PMMA-*b*-PSGMA), anionically synthesized and characterized as reported in detail elsewhere[14]. The copolymer is a hydrophobic (PMMA)–hydrophilic (polyelectrolytic PSGMA) diblock: $(CH_2\text{-}C(CH_3)CO_2CH_3)_{41}(CH_2\text{-}C(CH_3)CO_2\text{-}CH_2CHOHCH_2SO_3^-\ Na^+)_{115}$, where the polyelectrolytic block is 70% sulphonated. Control force versus distance measurements showed that, as expected, this negatively charged polymer does not adhere from aqueous solution to the bare negatively charged mica surface. Following hydrophobization of the surfaces and their incubation with the diblock, subsequent force profiles (Fig. 1) reveal clearly the attachment of the chains to the mica surfaces. The attachment must be via their hydrophobic PMMA moieties to form end-tethered layers of charged PSGMA moieties, as under these conditions the polyelectrolyte block, PSGMA, does not itself adsorb on hydrophobic surfaces[15]. The unperturbed thickness L of the PE brush is estimated from the profiles in Fig. 1 as $L = 13 \pm 2$ nm. Refractive index measurements on the confined PE layers revealed an adsorbance $\Gamma = 3 \pm 1\ \mathrm{mg\,m^{-2}}$ of the polymer on the hydrophobized mica, corresponding to a mean surface spacing between chains of 4 ± 0.7 nm.

The PE-brush-bearing mica surfaces were then progressively compressed, and the shear or frictional forces F_s between them measured as the top surface was made to slide back and forth past the lower one at increasing loads F_n and at different sliding velocities v_s. Typical results are shown in Fig. 2. Trace a in Fig. 2 shows the periodic lateral motion applied to the top mica surface, while traces b–d, taken directly from the recording oscilloscope, show the shear force transmitted to the lower surface across the interacting PE brushes at increasing compressions. The right inset in Fig. 2 shows the frequency dependence of the F_s responses in traces b–d, with arrows marking the signal at the drive frequency. Within the resolution of our apparatus, no systematic forces at the drive frequency (0.5 Hz for the traces shown) were measurable above the scatter $\delta F_s = \pm 20$–30 nN, up to loads corresponding to a mean pressure of a few atmospheres. We may define an effective friction coefficient $\mu_{\mathrm{eff}} = F_s/F_n$, where F_s is the force required to slide the surfaces past each other under a normal load F_n. At the higher loads before chain removal, where the mean pressure between the surfaces is $\sim 3 \times 10^5$ Pa, (as in trace c of Fig. 2, typical of other traces at these loads), $F_s \leq \delta F_s$ and we find $\mu_{\mathrm{eff}} \lesssim 0.0006$. Within the range of

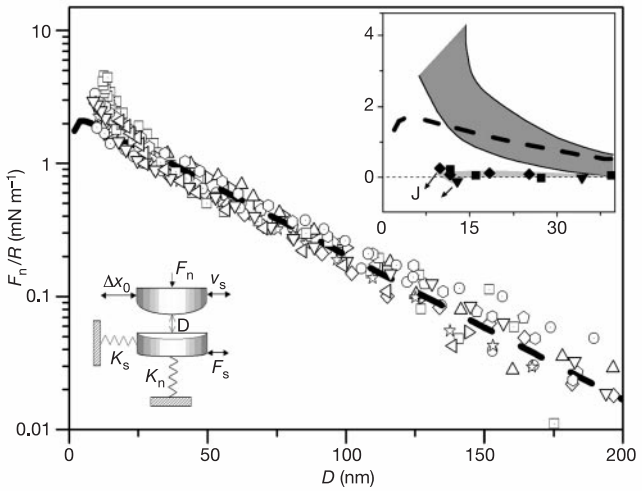

Figure 1 Force versus separation profiles. Normalized force ($F_n(D)/R$) versus surface separation (D) profiles between hydrophobized (STAI-coated) mica surfaces bearing PMMA-*b*-PSGMA diblock copolymers tethered by their PMMA moiety, where R is the mean radius of curvature of the surfaces. $D = 0$ refers to contact between bare mica surfaces in purified water. Profiles are taken following overnight incubation in $100 \pm 10\ \mu\mathrm{g\,ml^{-1}}$ PMMA-*b*-PSGMA aqueous solution. Results from different sets of experiments (different pairs of mica sheets) and different contact positions in each experiment, measured on first and second compression–decompression cycles, are shown. The broken curve is a fit to the DLVO expression[30] $F_n(D)/R = 128\pi c k_B T \kappa^{-1} \tanh^2(e\psi_0/4k_BT)\exp(-\kappa D) - A_H/6D^2$, where c is the ion concentration, T is the temperature (296 K), k_B is Boltzmann's constant, A_H is the Hamaker constant ($= 1.5 \times 10^{-20}$ J, the theoretical value for the interaction of two hydrocarbon-coated mica surfaces across water[4]), ψ_0 is the effective (far-field) surface potential, κ^{-1} is the Debye length (40 ± 3 nm, corresponding to a 1:1 ion concentration $c = (6 \pm 1) \times 10^{-5}$ M), and e is the electronic charge. The upper inset shows the data from the main figure at short separations on a larger scale (as a shaded band); from the deviation of the broken line from the data we estimate an unperturbed brush thickness of 13 ± 2 nm on each surface. The data points in the inset are the forces between the STAI-coated mica surfaces across water before incubation in the PMMA-*b*-PSGMA solution, showing the jump (at J) into strong adhesive contact. The lower inset shows schematically the SFB configuration, where K_s and K_n are the constants of the shear- and normal-force springs, respectively.

shear velocities studied, $250\,\mathrm{nm\,s^{-1}} < v_s < 500\,\mathrm{nm\,s^{-1}}$, the shear forces were, in all cases, within the noise level δF_s down to $D \approx 10$ nm. For this reason we could not determine a velocity or shear-rate dependence of the shear force, though the behaviour of the confined film in this regime was clearly liquid-like in the sense of not sustaining a yield stress. At the highest compressions, where the volume fraction of the compressed polymer was close to unity (for example, trace d in Fig. 2), a small shear force could be detected above the scatter just before the jump at J, from $D = 5.8 \pm 0.3$ nm into strong adhesive contact at $D = 1.9 \pm 0.3$ nm. In the adhesive contact following the jump the remaining confined film showed solid-like behaviour, in that a strong shear force was required before yield (sliding) was observed (right-hand side of trace d in Fig. 2).

We attribute this jump to an abrupt removal of the PE brush layers. As the top surface slides back and forth laterally, the surfaces approach slowly under thermal drift. The frictional drag between them grows, and some chains experience a force sufficient to overcome their hydrophobic adhesion to the STAI layers, causing them to detach. The shear force per chain on the remaining chains then becomes correspondingly larger, causing more of them to detach, and a rapid catastrophic removal of the diblocks occurs, leading to the jump observed at the point J (Fig. 2). It is of interest that the separation to which the surfaces jump is comparable with the double thickness of the hydrophobizing STAI layers[12,13], indicating the shear-off from the intersurface gap of most of the confined diblock. Such a shearing away of the PE brushes could be overcome by a more tenacious end-attachment of the PE moieties, such as by covalent tethering of the brush-chains to each surface, or endocytic anchoring for the case of PE layers at the outer surface of cell membranes. If the surfaces are separated from the adhesive contact following the PE shear-off, both the normal force profile and the very low friction, as well as the adsorbance revealed by refractive index measurements, recover to their equilibrium values (as in Figs 1 and 2, respectively) within 30 min.

These low values of the effective friction coefficient μ_{eff} reveal a remarkable capacity for lubrication by the PE brushes. We attribute this to two main factors. On the one hand, mutually compressed polymer brushes in a good solvent resist interpenetration, owing to excluded volume effects arising from chain configurational entropy[3,6,16–18]. Additionally, for the case of the PE brushes this configurational excluded volume effect is augmented by the large osmotic pressure exerted by mobile counterions within the brush[19–23], whose concentration, even in the unperturbed PE brushes, is ~0.3 M. This implies that a given load can be supported with less mutual interpenetration than for neutral brushes[20], thereby reducing the extent of the sheared interfacial region when the opposing surfaces slide past each other. Indeed, an estimate of the extent of mutual interpenetration of the brushes in our system (U.R. *et al.*, manuscript in preparation), based on the arguments of ref. 16 together with the calculations in ref. 22, suggests this is no more than ~1 nm at the highest compressions before shear-off of the brushes. At the same time, each of the charged PE segments rubbing against others within the sheared interpenetration zone is surrounded by a hydration sheath. As has recently been demonstrated, such sheaths are tenaciously bound to the charges but are at the same time very fluid, and so serve as efficient lubricating layers[8].

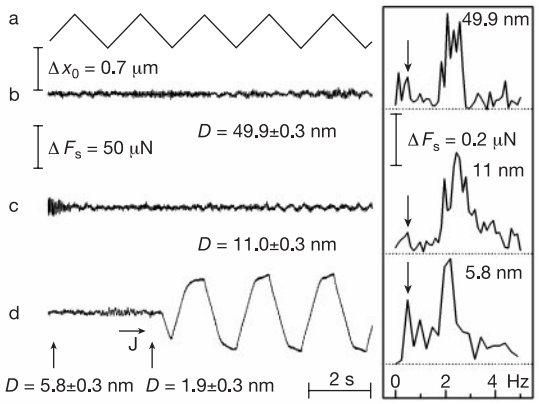

Figure 2 Frictional forces between PE brushes. Main panel; traces show the shear forces F_s between STAI-coated mica surfaces bearing the PMMA-*b*-PSGMA brushes in conductivity water, as they slide past each other at different surface separations D, and are taken directly from the recording oscilloscope. Trace a shows the lateral back-and-forth lateral motion (Δx_0, lower inset to Fig. 1) applied to the top mica surface. Traces b–d show the corresponding shear force F_s transmitted between the surfaces at the surface separations indicated. Frequency analysis (inset, right) reveals that the magnitude of F_s at the frequency of the lateral drive motion (0.5 Hz, indicated by arrows) for a surface separation $D = 11$ nm (trace c) is, within the noise-limiting sensitivity ($\delta F_s = \pm 30$ nN), indistinguishable from its value at large separations (trace b, $D = 49.9$ nm). In trace d the surfaces have been further compressed and, just before jump-in at the point J, from $D = 5.8 \pm 0.3$ nm to $D = 1.9$ nm (when the PE brushes are sheared off, see text), the shear force at the drive frequency increases to $F_s(0.5\,\mathrm{Hz}) = 200 \pm 30$ nN. The mean pressure between the surfaces is given by $P = F_n(D)/A$, where F_n is the load and the area A may be evaluated from hertzian contact mechanics[4]. For $D = 5.8$ nm (trace d before jump-in), $P = 3 \times 10^5\,\mathrm{N\,m^{-2}}$. Very similar traces to d (not shown) were obtained in other runs just before shear-off of the brushes.

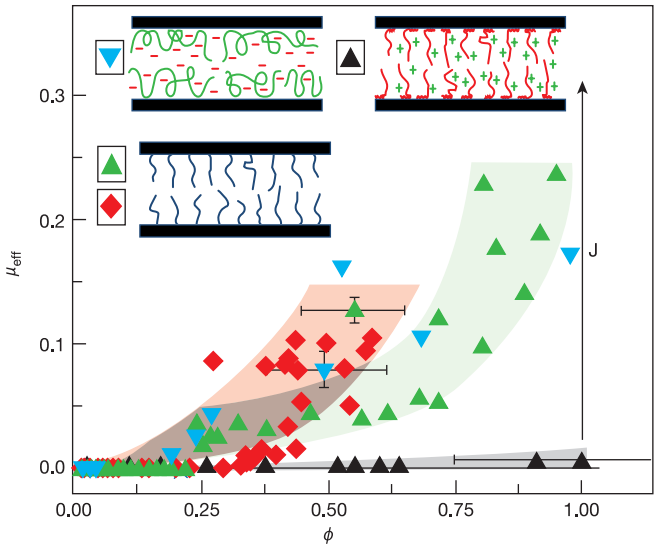

Figure 3 Variation of the effective friction coefficient μ_{eff} with volume fraction ϕ of confined polymer for different polymer lubricants. Volume fractions are based on absolute adsorbance values determined for the respective polymers from *in situ* refractive index measurements. Red and green symbols are for neutral brushes in non-polar[5] and in aqueous[24] good solvents respectively, with respective bands indicating the range of the scatter. Blue symbols are for an adsorbed cationic polyelectrolyte, chitosan, in an aqueous solution at pH 3.5 (ref. 31); the normal force profiles of this chitosan sample, $M = 6 \times 10^5$ and degree of deacetylation 85% (Fluka), are very similar to those reported in ref. 28 where a comparable chitosan sample was used in similar conditions. The adsorbance of our chitosan sample onto each mica surface is $1.2\,\mathrm{mg\,m^{-2}}$, determined by *in situ* refractive index measurements. The data shown are from two independent experiments and different contact points within each experiment). The black symbols and corresponding grey band are from the present study on the PMMA-*b*-PSGMA brushes. Shear velocities for all data are in the range 250–500 nm $\mathrm{s^{-1}}$. The cartoons illustrate the different charged and uncharged polymer lubricant configurations, with positive or negative charge signs indicating the counterions.

Refinement of the above model will require more detailed investigation of how the shear and normal forces vary with PE length, charge density, adsorbance and attachment to the surface, as well as with salt concentration in the surrounding aqueous medium.

As this combination of charge and steric effects is absent in most other forms of polymeric surfactant, it is instructive to compare the frictional effects for different classes of solvated polymer surface layers. These include neutral brushes in both aqueous[24] and organic[5–7] liquids, and adsorbed (as opposed to end-tethered) neutral[25] and charged polymers. Many different measures for such a comparison are clearly possible, even when limiting ourselves to frictional studies using the standard SFB configuration. A particularly useful measure at high compressions—the most interesting regime—which acts to normalize effects due to the different surface architectures, surface densities and layer thicknesses, is to examine how μ_{eff} varies with the volume fraction ϕ of the compressed polymer layers. This is because volume fractions of the compressed polymers are directly related to the pressure between the surfaces, but primarily because at the high volume fractions corresponding to the strongest compressions, these pressures become independent of the details of the polymer conformations[26]. The osmotic pressures supporting the load between the rubbing surfaces then depend—in a good solvent—on the monomer concentrations[26]. At the same time, for an unentangled interpenetration zone, the viscous dissipation within the sheared layer depends—for a given shear rate and concentration—on the monomeric friction alone[16,27].

In Fig. 3 we compare the present results on PE brushes with frictional SFB studies on other generic cases, at comparable shear velocities: neutral brushes in an organic solvent[5] and in water[24], and an adsorbed charged polymer (chitosan) in aqueous solution[28] (N.K., U.R. and J.K., unpublished data), all in good solvent conditions. The effective friction coefficient μ_{eff} defined earlier is plotted against the volume fraction ϕ of the compressed, sheared polymers. All polymer surfactants lead to very low effective friction coefficients at volume fractions $\phi \lesssim 0.3$. But whereas the neutral brushes and the adsorbed charged chains (coloured symbols and bands in Fig. 3) show a rapid increase in μ_{eff} at higher volume fractions, friction mediated by PE brushes (black symbols and grey band) remains extremely low up to the point of brush removal J (by which point the volume fraction is, within the scatter, close to unity). For the neutral brushes in aqueous and organic solvents[5–7,24], this increase has been attributed largely to the sharp increase in the effective viscosity of the sheared interfacial region at the higher ϕ values, together with the greater mutual interpenetration of the opposing layers at the higher loads. For the adsorbed PE chain (blue symbols in Fig. 3), where counterion osmotic effects and lubricating hydration sheaths are expected to be similar to those acting in the PE brush, the origin of the rapid increase in the friction may be different, and associated rather with bridging effects. This effect, suggested also to explain the higher frictional drag between neutral adsorbed chains relative to neutral polymers brushes[25] and in other studies of adsorbed PE[29], arises when chains bridge the gap to adsorb simultaneously on both sliding surfaces. Bridging is absent for polymer brushes, which do not adsorb but are end-attached to the surface. The fact that, in contrast to all the other cases, the PE brushes uniquely retain their extreme propensity for lubrication even at volume fractions approaching unity, is compelling. It supports the notion that it is the counterion-induced PE-brush swelling, together with the fluid hydration sheaths about the charged segments and absence of bridging effects, that are effective in overcoming the factors leading to larger frictional dissipation for all other types of polymeric lubricants studied.

It is tempting to consider the relevance of this finding for other systems, particularly in nature, where charged polymers at biological surfaces are ubiquitous. In the experiments reported here water at very low salt concentration was used, but we note that preliminary results with added salt (to concentration $\sim 10^{-2}$ M) show that the frictional forces remain extremely weak ($\mu_{\mathrm{eff}} \lesssim 10^{-3}$), up to comparably high pressures. This salt concentration is still lower than the value ($\sim$0.1 M) pertaining in physiological conditions. However, the concentration of ionized monomers and the compensating free counterions within the PE brush can be easily comparable or larger than this when the brushes are highly compressed. This suggests that lubrication in living systems may be mediated by brush-like PE lubricants. □

Received 20 April; accepted 5 August 2003; doi:10.1038/nature01970.

1. Napper, D. H. *Polymeric Stabilization of Colloidal Dispersions* (Academic, London, 1983).
2. Dowson, D. (ed.) *Proc. Inst. Mech. Eng. H* Vol. 201 (special issue on biolubrication) 189–247 (1987).
3. de Gennes, P. G. Polymers at an interface: A simplified view. *Adv. Colloid Interface Sci.* **27,** 189–207 (1987).
4. Israelachvili, J. N. *Intermolecular and Surface Forces* (Academic, London, 1992).
5. Klein, J., Kumacheva, E., Mahalu, D., Perahia, D. & Fetters, L. Reduction of frictional forces between solid surfaces bearing polymer brushes. *Nature* **370,** 634–636 (1994).
6. Grest, G. S. Normal and shear forces between polymer brushes. *Adv. Polym. Sci.* **138,** 149–182 (1999).
7. Kilbey, S. M. II, Schorr, P. A. & Tirrell, M. in *Dynamics of Small Confining Systems IV* (eds Drake, J. M., Grest, G. S., Klafter, J. & Kopelman, R.) 181–187 (Materials Research Society, Pittsburgh, PA, 1999).
8. Raviv, U. & Klein, J. Fluidity of bound hydration layers. *Science* **297,** 1540–1543 (2002).
9. Klein, J. & Kumacheva, E. Simple liquids confined to molecularly thin layers. I. Confinement-induced liquid to solid phase transitions. *J. Chem. Phys.* **108,** 6996–7009 (1998).
10. Pashley, R. M. Hydration forces between mica surfaces in aqueous electrolyte solutions. *J. Colloid Interface Sci.* **80,** 153–162 (1981).
11. Raviv, U., Laurat, P. & Klein, J. Fluidity of water confined to sub-nanometre films. *Nature* **413,** 51–54 (2001).
12. Tadmor, R., Rosensweig, R. E., Frey, J. & Klein, J. Resolving the puzzle of ferrofluid dispersants. *Langmuir* **16,** 9117–9120 (2000).
13. Raviv, U., Giasson, S., Frey, J. & Klein, J. Viscosity of ultra-thin water films confined between hydrophobic or hydrophilic surfaces'. *J. Phys. Condens. Matter* **14,** 9275–9283 (2002).
14. Gohy, J. F., Antoun, S. & Jerome, R. Self-aggregation of PMMA-b-PSGMA copolymers. *Polymer* **42,** 8637–8645 (2001).
15. Abraham, T., Giasson, S., Gohy, J.-F., Jerome, R. & Stamm, M. Adsorption kinetics of a hydrophobic-hydrophilic diblock polyelectrolyte at the solid-aqueous solution interface. *Macromolecules* **33,** 6051–6059 (2000).
16. Witten, T., Leibler, L. & Pincus, P. Stress-relaxation in the lamellar copolymer mesophase. *Macromolecules* **23,** 824–829 (1990).
17. Wijmans, C. M., Zhulina, E. B. & Fleer, G. J. Effect of free polymer on the structure of a polymer brush and interaction between 2 polymer brushes. *Macromolecules* **27,** 3238–3248 (1994).
18. Klein, J. Shear, friction, and lubrication forces between polymer-bearing surfaces. *Ann. Rev. Mater. Sci.* **26,** 581–612 (1996).
19. Miklavic, S. J. & Marcelja, S. Interaction of surfaces carrying grafted polyelectrolytes. *J. Phys. Chem.* **92,** 6718–6724 (1988).
20. Pincus, P. Colloid stabilization with grafted polyelectrolytes. *Macromolecules* **24,** 2912–2919 (1991).
21. Misra, S., Tirrell, M. & Mattice, W. Interaction between polyelectrolyte brushes in poor solvents. *Macromolecules* **29,** 6056–6060 (1996).
22. Borisov, O. B., Zhulina, E. B. & Birshtein, T. M. Diagram of states of a grafted polyelectrolyte layer. *Macromolecules* **27,** 4795–4803 (1994).
23. Csajka, F. S., Netz, R. R., Seidel, C. & Joanny, J.-F. Collapse of polyelectrolyte brushes: Scaling theory and simulations. *Eur. Phys. J. E* **4,** 505–513 (2001).
24. Raviv, U. *et al.* Properties and interactions of physigrafted end-functionalised poly(ethylene glycol) layers. *Langmuir* **18,** 7482–7495 (2002).
25. Raviv, U., Tadmor, R. & Klein, J. Shear and frictional interactions between adsorbed polymer layers in a good solvent. *J. Phys. Chem. B* **105,** 8125–8134 (2001).
26. de Gennes, P. G. *Scaling Concepts in Polymer Physics* (Cornell Univ. Press, Ithaca, NY, 1979).
27. Ferry, J. D. *Viscoelastic Properties of Polymers*, 3rd edn (Wiley, New York, 1985).
28. Claesson, P. M. & Ninham, B. W. pH dependent interactions between adsorbed chitosan layers. *Langmuir* **8,** 1406–1412 (1992).
29. Ruths, M., Sukhishvili, S. A. & Granick, S. Static and dynamic forces between adsorbed polyelectrolyte layers (quaternized poly-4-vinylpyridine). *J. Phys. Chem. B* **105,** 6202–6210 (2001).
30. Derjaguin, B. V., Churaev, N. V. & Muller, V. M. *Surface Forces* (Plenum, New York, 1987).
31. Kampf, N., Raviv, U. & Klein, J. Normal and shear forces between adsorbed and gelled layers of chitosan, a naturally occurring cationic polyelectrolyte. *Macromolecules* (submitted).

Acknowledgements We thank J. Frey for the STAI synthesis, and R. Tadmor, T. Witten, D. Lukatsky and P. Pincus for discussions. We also thank the Eshkol Foundation (U.R.), the Canadian Friends of the Weizmann Institute (Charpak-Vered Fellowship, S.G.), the US-Israel BSF, the Deutsche-Israelische Program, and the Israel Science Foundation for their support of this work. J.F.G. (Chargé de Recherches by FNRS) and R.J. thank the SSTC for financial support.

Competing interests statement The authors declare that they have no competing financial interests.

Correspondence and requests for materials should be addressed to J.K. (jacob.klein@weizmann.ac.il or jacob.klein@chem.ox.ac.uk) or S.G. (suzanne.giasson@umontreal.ca)